Eur. Phys. J. D **11**, 197–205 (2000)

THE EUROPEAN PHYSICAL JOURNAL D

EDP Sciences

Finestructure, hyperfine structure and isotope shift of $4f^{12}6s7s$ in Er I

D. Ashkenasi[1,a], S. Kröger[2,b], and H.-D. Kronfeldt[3,c]

[1] Max Born Institut für Nichtlineare Optik und Kurzzeitspektroskopie, Rudower Chaussee 6, 12489 Berlin, Germany
[2] Institut für Atomare und Analytische Physik, Technische Universität Berlin, Hardenbergstr. 36, 10623 Berlin, Germany
[3] Optisches Institut, Technische Universität Berlin, Hardenbergstr. 36, 10623 Berlin, Germany

Received 16 May 1999 and Received in final form 31 January 2000

Abstract. The isotope shift (IS) and hyperfine structure (hfs) of nine levels (31720 to 38921 cm^{-1}) assigned to the configuration $4f^{12}6s7s$ in neutral erbium have been determined experimentally using Doppler-reduced saturation absorption spectroscopy in a gas discharge. We performed a fine structure analysis in the SL-coupling scheme of the single configuration $4f^{12}6s7s$, confirming and extending the classification of even parity Er I levels. We discriminated the different hfs contributions of the $4f^{12}$ core and the $(6s+7s)$ outer electrons of the shell in a non-relativistic JJ-coupling approach and in the relativistic effective tensor operator formalism in SL-coupling. The relativistic one-electron parameters of the hfs for ^{167}Er were fitted to the experimental data by a least squares fit procedure: $a^{01}_{4f} = -147(3)$ MHz, $a^{10}_{6s} + a^{10}_{7s} = -1840(30)$ MHz, $b^{02}_{4f} = 6560(80)$ MHz. The level dependencies of the isotope shift were evaluated based on crossed second order (CSO) effects. We obtained the following results for the CSO parameters for the isotope pairs $^{170-168}$Er: $d_{6s7s} = -740(30)$ MHz, $z_{4f} = 0(5)$ MHz, $(g_{3,6s}(f,6s) + g_{3,7s}(f,7s)) = -24(15)$ MHz and for $^{170-166}$Er: $d_{6s7s} = -1500(50)$ MHz, $z_{4f} = 0(10)$ MHz, $(g_{3,6s}(f,6s) + g_{3,7s}(f+7s)) = -50(29)$ MHz. The resulting parameters for the hfs are compared with those known for other configurations of the Er atom and ion.

PACS. 21.10.Ky Electromagnetic moments – 31.30.Gs Hyperfine interactions and isotope effects, Jahn-Teller effect – 32.10.Fn Fine and hyperfine structure

1 Introduction

On the basis of the non-relativistic wave functions in the SL-coupling scheme, the hyperfine structure (hfs) can be treated within the effective tensor operator formalism. Briefly, the hfs constants – magnetic dipole A and electric quadrupole B – are expressed as a linear combination of their relativistic one-electron hfs parameters $a^{k_s}_{nl}$ and $b^{k_s k_l}_{nl}$ [1,2]. Trends of the corresponding effective electronic radial integrals along the element series, *i.e.* the lanthanides, are discussed to obtain a stronger insight towards the complex multi-body problem [3]. A similar effort can be seen in the evaluation of the isotope shift (IS). Term and level (J-) dependencies in the IS within one configuration are interpreted as crossed-second-order (CSO) effects [4,5].

However, most of the detailed evaluation on the hfs and IS concentrates on configurations in the lower energetic range, *e.g.* the ground configuration or the lowest lying configuration of opposite parity. A complete atomic evaluation of high lying levels is fairly rare, mainly because of the following reasons: the lower levels of the transitions in the visible are not metastable making high resolution spectroscopy more challenging and, perhaps even more important, high-lying levels usually contain admixtures of states from many other configurations, making a meaningful theoretical interpretation very difficult.

The general remarks made above hold true for most of the investigations in the lanthanide element series. Atomic studies in Er, a highly refractory element, were performed for the even parity ground configuration $4f^{12}6s^2$ [6–8] and the lowest odd parity ground configuration $4f^{11}5d6s^2$ [9,10]. Wyart [9] calculated eigenvectors of the low lying odd parity levels in the system $4f^{11}(^4I)5d6s^2 + 4f^{12}6s6p + 4f^{11}(^4I)5d^26s$, so that configuration mixing could have been included in the evaluation of the hfs in $4f^{11}5d6s^2$. However, the interpretation of the atomic effects was based only on the purest low-lying levels, indicating the difficulties which arise due to an incomplete description of the configuration mixing. Standard laser induced fluorescence in an optically excited atomic beam combined with a magnetic-dipole radio-frequency transition, *i.e.* a double-resonance technique, was used by Childs *et al.* [7,10] to investigate several Er I transitions. Though, the application

[a] e-mail: ashke@mbi-berlin.de
[b] e-mail: sk@kalium.physik.tu-berlin.de
[c] e-mail: kf@mail.physik.tu-berlin.de

of this precise method is restricted to metastable lower levels.

Saturation absorption spectroscopy (SAS) in a gas discharge has been cultivated in a recent study for the higher even parity Er I configuration $4f^{11}5d6s6p$ [11], where various investigated transitions started from non-metastable levels of the $4f^{11}5d6s^2$ configuration. This study in Er I, together with investigations performed for the equivalent configurations $4f^n5d6s6p$ in Gd [12], Ho [13] and Yb [14], demonstrates that one can obtain a very reasonable relativistic hfs-description even in an energetically high lying and complex electronic system with up to four open shells.

Several strong Er I transitions between the configurations $4f^{12}6s6p$ and $4f^{12}6s7s$ [15] argue that the high lying even parity configuration is adequately free from configuration mixing [16]. High resolution investigation of these transitions in Er I is therefore most attractive, since this configuration serves as an ideal test ground for a complete evaluation of the fs, hfs and IS in a high lying configuration. We were also interested to study possible tendencies of the IS and hfs in $4f^n6s7s$, extending recent investigations on similar electronic systems, such as $4f^{13}6s7s$ of Tm I [17] and $4f^76s7s$ of Eu I [18] inside the lanthanide element series.

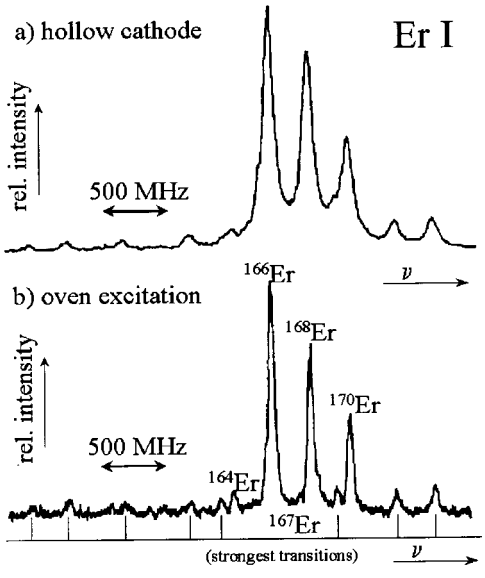

Fig. 1. Saturation absorption signal of Er I transition 660.11 nm (17074–32219 cm^{-1}): (a) using a high-current hollow-cathode gas discharge lamp; (b) using an atom oven source with a discharge above the tantalum oven orifice.

2 Experiment

The Doppler-reduced measurements were carried out by means of saturation absorption spectroscopy (SAS) in a discharge containing Er I in its natural abundance. Details of the experimental set-up can be found *e.g.* in [12,19]. We used two different atomic sources for the SAS experiments, a high-current hollow cathode and a modified atomic oven. Figure 1 illustrates a SAS profile of the weak Er transition at $\lambda = 660.11$ nm using a self-constructed hollow-cathode (top picture) and an atomic oven including a discharge for permanent excitation (lower picture). The lower non-metastable level $4f^{12}6s6p$ at 17074 cm^{-1} of this transition demonstrates a very strong decay to the ground configuration. This situation was typical for most of the transitions investigated in this work, as compiled in Table 1. For a complete evaluation of the level isotope shift is was necessary to include some of the fairly weak transitions in this study.

The self-constructed see-through hollow cathode was demountable and water-cooled [12]. The discharge current between the stainless steel anode and the Er hollow cylinder cathode was set between 0.5 and 1.0 A at a voltage of around 250 V. The buffer-gas atmosphere chosen for the investigations was a Ar–Kr mixture (ratio typically 1 to 1) of a pressure between 40 and 120 Pa. A common artifact in SAS are Doppler-pedestals underlying the Lorentzian shaped signal part. The Doppler-pedestal contribution in the total signal can be very dominating in some cases, especially for transitions with metastable lower levels. Cause of this effect are velocity-changing collisions during the "pump-probe" modulation time [20,21]. However, the high discharge current reduced the Doppler contribution in the spectra below 10%, as can be seen

Table 1. Er I transitions of the type $4f^{12}6s6p$ to $4f^{12}6s7s$, $4f^{11}5d^26s$ to $4f^{12}6s7s$ and $4f^{12}6s^2$ to $4f^{12}6s6p$ investigated in this work. Notation and energy (in cm^{-1}) are taken from [16]. The estimated visual intensities *e.v.i.* and wavelengths are taken from [15].

Wavelength	Odd Parity			Even Parity			*e.v.i*
nm	Energy	Notation		Energy	Notation		
	Configuration $4f^{12}6s6p$			Configuration $4f^{12}6s7s$			
		J_1, J_2	J		J_1, J_2	J	
628.859	16321.110	6,0	6	32218.588	6,1	5	200
639.813	16321.110	6,0	6	31946.417	6,1	6	300
649.235	16321.110	6,0	6	31719.664	6,1	7	500
660.111	17073.800	6,1	6	32218.588	6,1	5	600
672.191	17073.800	6,1	6	31946.417	6,1	6	15000
682.598	17073.800	6,1	6	31719.664	6,1	7	8000
675.987	17157.307	6,1	7	31946.417	6,1	6	20000
684.811	17347.860	6,1	5	31946.417	6,1	6	80000
646.540	21551.919		4	37014.608	4,1	4	60
652.052	21551.919		4	36883.886	4,1	5	400
677.337	22124.268		5	36883.886	4,1	5	4000
672.100	22269.457		3	37144.092	4,1	3	1500
678.003	22269.457		3	37014.608	4,1	4	250
676.292	22361.651		4	37144.092	4,1	3	2000
648.174	23447.079		5	38870.770	5,1	6	400
646.063	23447.079		5	38921.185	5,1	4	200
664.896	23885.406		5	38921.185	5,1	4	2000
682.544	24246.146		6	38893.172	5,1	5	4000
683.590	24246.146		6	38870.770	5,1	6	150
687.366	24348.910		4	38893.172	5,1	5	250
	Configuration $4f^{11}5d6s^2$						
638.819	16070.095	13/2,3/2	6	31719.664	6,1	7	300
	Configuration $4f^{12}6s6p$			Configuration $4f^{12}6s^2$			
					^{2S+1}L	J	
591.646	23855.654		5	6958.329	^3H	5	80
590.606	23885.406		5	6958.329	^3H	5	300
575.235	28129.803		5	10750.982	^3H	4	80
587.163	27777.315		4	10750.982	^3H	4	60

Table 2. (a) Experimental hyperfine splitting constants $A_{\rm exp}$ and $B_{\rm exp}$ of even parity levels in the configuration $4f^{12}6s7s$ with uncertainty (standard deviation) in brackets. (b) Experimental hyperfine splitting constants $A_{\rm exp}$ and $B_{\rm exp}$ of odd parity levels of the configuration $4f^{12}6s6p$ with uncertainty (standard deviation) in brackets.

(a)

level energy cm^{-1}	J	$A_{\rm exp}$ MHz	$B_{\rm exp}$ MHz
31719.664	**7**	**-230.91 (14)**	**-4195 (6)**
31946.417	**6**	**-161.99 (13)**	**-3806 (11)**
32218.588	**5**	**19.1 (3)**	**-4017 (10)**
36883.886	**5**	**-263.4 (6)**	**21 (3)**
37014.608	**4**	**-163.4 (2)**	**-110 (40)**
37144.092	**3**	**100.2 (1.1)**	**250 (30)**
38870.770	**6**	**-279.2 (8)**	**-3950 (30)**
38893.172	**5**	**-170.1 (8)**	**-3585 (17)**
38921.185	**4**	**0.0 (2)**	**-3440 (50)**

(b)

level energy cm^{-1}	J	$A_{\rm exp}$ MHz	$B_{\rm exp}$ MHz
23447.079	**5**	**-173.3 (4)**	**-2836 (25)**
23855.654	**5**	**-216.7 (1.1)**	**-3448 (30)**
23885.406	**5**	**-176.3 (1.0)**	**-1773 (30)**
24348.910	**4**	**-125.6 (1.7)**	**-2599 (9)**
27777.315	**4**	**-138 (3)**	**-870 (15)**

in Figure 1a. High frequency modulation technique, as suggested in [21], to completely eliminate the Doppler background in the SAS signal was not necessary in this case. A increasing in buffer-gas pressure resulted in an additional Lorentzian line-width of around 0.6 MHz/Pa, *e.g.* from typically 70 MHz (FWHM) at 40 Pa to 100 MHz at 120 Pa. However, a higher noble-gas pressure led to a much improved signal to noise ratio in the SAS-spectra, which was especially important for some of the weaker transitions.

The experimental intensity distributions of the transitions in Table 1 were fitted by theoretically reproducing the complete SAS spectra, varying the atomic constants and the line shape parameters, but keeping the isotope abundance and the relative intensities of the hfs components constant. The experimental resolution of 40–100 MHz (FWHM) and program fitting routine enabled a complete determination of the relative positions of the four even isotopes ^{170,168,166,164}Er with a typical uncertainty of 1–3 MHz. With similar precision we were able to determine the relative centre of gravity of the only stable odd isotope ^{167}Er, of which the strongest hyperfine components were in most cases easy to identify. The experimentally determined hfs-constants, A and B, of the nine levels of the configuration $4f^{12}6s7s$ are compiled in Table 2a. Note also the hfs constants for several non-metastable levels in the configuration $4f^{12}6s6p$ given for the first time in Table 2b.

For a few of the stronger transitions it was possible to obtain a SAS-signal of low noise level with a modified atomic beam source, formally used for laser induced fluorescence measurements of transitions from metastable lower levels [22]. For excitation of these metastable levels an iron spiral is placed about 5 mm above the Ta-oven which is filled with Er-pellets. In the Er vapor cloud forming above the Ta-oven a discharge was ignited (DC voltage between iron spiral and oven about 600 V, current up to 600 mA). The SAS profile of the transition at $\lambda = 660.11$ nm in Figure 1b demonstrates the improvement in resolution using the oven discharge source, as pressure broadening could be minimized. The Lorentzian line-widths remained below 40 MHz (FWHM). Any former Doppler contribution due to collisions in the background gas is practically eliminated in this collimated atomic oven source.

3 Results and discussion

3.1 Fine structure

A preliminary investigation of the fine structure (fs) for the configuration $4f^{12}6s7s$ was accomplished by Wyart, van Kleef and Koot. Their unpublished results on $4f^{12}6s7s$ as well as the unpublished work on the system $4f^{11}6s^26p + 4f^{12}5d6s$ served as basis for the assignment of the Er levels in [16]. Also, fs calculations were performed for even parity levels in Er I only for $4f^{12}6s^2$ [6] and recently for $4f^{11}5d6s6p$ [11]. An overwhelming part of even parity levels in the energy range above 33000 cm^{-1} remained still unclassified. The reason for this theoretical gap lies in the fact that the fs calculations for $4f^{11}6s^26p + 4f^{12}5d6s$ and $4f^{11}5d6s6p$ were restricted to the ^4I core of $4f^{11}$. Therefore, the fs description for higher even parity levels is a point at issue. However, the high lying configuration $4f^{12}6s7s$ seems fairly pure and well described in a single-configuration fs calculation. From altogether 48 theoretical fs levels 18 are apparently identified in this configuration [16].

In this work, we reexamined the Er I levels in $4f^{12}6s7s$ by performing a single-configuration fs-calculation in the SL-coupling scheme $\{4f^{12}(^{2S_1+1}L_1)6s7s(^{1,3}S)\}^{2S+1}L$ to obtain the wave functions for an interpretation of the IS and hfs. For the semi-empirical approach altogether 11 fs parameters were applied. Table 3 compiles the resulting fs-parameters. Three fs-parameters, α, β and γ, remained fixed. Additionally, two pairs of fs-parameters were held at a constant ratio: $E^2 = E^1/217$, taken from Er I $4f^{11}5d6s^2$ [9] and $G^3(4f, 7s) = G^3(4f, 6s)/6$, taken from Eu I $4f^76s7s$ [18]. Unfortunately, it was not possible to determine the fs-parameter $G^3(4f, 7s)$ independently. The quality of the fs-fit remained the same for the ratios $G^3(4f, 6s)/G^3(4f, 7s)$ between 2 and 20. The difficulty in determining the $7s$ contribution in the fs is very typical inside the lanthanide series, particularly, when the number of known levels, assigned to singlet states (^1S) of $6s7s$ is very small (here: only one).

Table 4 finally compiles the experimental and theoretical energy levels of the configuration under investigation up to 45000 cm^{-1}. The standard deviation of the energy fit is 72 cm^{-1}. Only one level could be assigned

Table 3. Fine structure parameters for the even configuration $4f^{12}6s7s$ in Er I from a fit to the experimental level energies. *: Kept in a constant ratio to the previous parameter, based on previous calculations in Eu I. **: Kept constant.

fs-parameter	value [cm^{-1}]
E_{av}	45060 (200)
E^1	6650 (110)
E^2 *	30
E^3	615 (6)
$G^3(4f,6s)$	1320 (170)
$G^3(4f,7s)$ *	220
$G^0(4f,6s)$	810 (40)
ζ_{4f}	2247 (11)
a **	10
β **	100
γ **	-50

Table 4. Experimental ($E_{\rm exp}$) and calculated ($E_{\rm calc}$) energy levels, experimental ($g_{\rm exp}$) and calculated ($g_{\rm calc}$) g-factors and two leading components in LS-coupling with percentage contribution of identified and 4 theoretical levels in the Er I configuration $4f^{12}6s7s$; Δ: deviation between experimental and calculated energy level.

E_{exp} cm^{-1}	$E_{calc.}$ cm^{-1}	Δ cm^{-1}	$g_{exp.}$	$g_{calc.}$	two leading components in LS-coupling $^{(2S_1+1)}L_1$		$^{(2S_{23}+1)}L_{23}$ $^{(2S+1)}L$	
$J=1$						%		%
44 886.482	44 872	14	0.105	0.101	$^3F\,^3S\,^5F$	82	$^1D\,^3S\,^3D$	17
$J=2$								
44 347.866	44 274	74	0.870	0.853	$^3F\,^3S\,^5F$	54	$^3F\,^3S\,^3F$	44
45 060.489	45 024	37	0.850	0.872	$^3F\,^3S\,^3F$	48	$^3F\,^3S\,^5F$	33
$J=3$								
37 144.092	37 233	-89	0.890	0.930	$^3F\,^3S\,^3F$	31	$^1G\,^3S\,^3G$	27
42 611.413	42 676	-64	0.705	0.675	$^3H\,^3S\,^5H$	64	$^3F\,^3S\,^3F$	13
44 309.935	44 232	77	1.150	1.190	$^3F\,^3S\,^5F$	75	$^3F\,^3S\,^1F$	24
45 246.857	45 180	66	1.105	1.120	$^3F\,^3S\,^3F$	39	$^3F\,^3S\,^1F$	30
$J=4$								
37 014.608	37 096	-81	1.135	1.194	$^3F\,^3S\,^3F$	39	$^3F\,^3S\,^5F$	26
-	38 686	-	-	1.139	$^3F\,^1S\,^3F$	64	$^1G\,^1S\,^1G$	8
38 921.185	38 920	1	0.855	0.855	$^3H\,^3S\,^3H$	54	$^3H\,^3\,^5H$	42
42 681.708	42 741	-60	1.010	0.986	$^3H\,^3S\,^5H$	35	$^3H\,^3S\,^3H$	29
-	44 193	-	-	1.262	$^3F\,^3S\,^5F$	50	$^3F\,^3S\,^3F$	38
-	44 401	-	-	0.974	$^3H\,^1S\,^3H$	57	$^3F\,^1S\,^3F$	22
$J=5$								
32 218.588	32 140	78	1.050	1.028	$^3H\,^3S\,^3H$	49	$^3H\,^3S\,^1H$	37
36 883.886	36 942	-58	1.255	1.325	$^3F\,^3S\,^5F$	68	$^1G\,^3S\,^3G$	25
38 893.172	38 884	9	1.045	1.034	$^3H\,^3S\,^5H$	66	$^3H\,^3S\,^1H$	33
-	40 489	-	-	1.034	$^3H\,^1S\,^3H$	100		
42 736.803	40 489	-98	1.095	1.139	$^3H\,^3S\,^3H$	32	$^3F\,^3S\,^5F$	22
$J=6$								
31 946.417	31 907	40	1.195	1.186	$^3H\,^3S\,^3H$	54	$^3H\,^3S\,^5H$	44
33 519.739	33 523	-3	1.180	1.166	$^3H\,^1S\,^3H$	98	$^3H\,^3S\,^5H$	1
38 870.770	38 854	16	1.180	1.193	$^3H\,^3S\,^5H$	55	$^3H\,^3S\,^3H$	45
$J=7$								
31 719.664	31 678	41	1.285	1.285	$^3H\,^3S\,^5H$	99	$^1I\,^3S\,^3I$	1

Table 5. Experimental line isotope shifts with uncertainty (standard deviation) in brackets for all lines listed in Table 1 compiled for altogether four different Er isotope pairs: $^{170-168}$Er, $^{170-167}$Er, $^{170-166}$Er, and $^{170-164}$Er.

Wavelength	Experimental line isotope shift in MHz			
nm	170-168	170-167	170-166	170-164
628,8588	-336 (4)	-554 (7)	-665 (10)	-1000 (10)
639,8133	-287 (8)	-474 (8)	-568 (4)	-845 (12)
649,2351	-288 (2)	-492 (2)	-567,2 (1,8)	-840 (4)
660,1110	393 (3)	652 (3)	779,6 (1,4)	1163 (7)
672,1910	443 (5)	731,2 (1,7)	875 (5)	1249 (10)
682,5977	445 (8)	738 (15)	878 (5)	1325 (20)
675,9871	445,0 (1,0)	737 (2)	878,8 (1,9)	1323 (5)
684,8105	447 (4)	747,3 (1,9)	895,6 (1,3)	1354 (5)
652,0519	696 (2)	1166 (5)	1376,8 (1,5)	2041 (3)
677,3373	505 (4)	830 (5)	1000 (4)	1501 (10)
672,1004	414 (8)	678 (10)	810 (8)	1231 (20)
678,0027	843 (2)	1399 (4)	1665 (3)	2512 (8)
676,2919	138,7 (1,9)	232 (6)	279,9 (1,0)	395 (4)
648,1742	456 (5)	757 (5)	907 (3)	1370 (6)
646,0629	490 (3)	814 (5)	972 (4)	1462 (8)
664,8963	495 (3)	821 (5)	983 (3)	1474 (10)
682,5435	503 (3)	836 (6)	999 (3)	1499 (10)
683,5902	485 (2)	806 (8)	980 (5)	1445 (10)
687,3660	525,7 (1,3)	874 (2)	1044 (2)	1574 (7)
638,8186	-972 (2)	-1635 (5)	-1921 (4)	-2890 (7)
591,646	-1029 (6)	-1591 (6)	-2045 (6)	-2844 (8)
590,606	-1099 (4)	-1754 (6)	-2179 (5)	-3218 (7)
575.235	-865 (5)	-1382 (5)	-1710 (6)	-2601 (6)
587.163	-1002 (4)	-1596 (10)	-1949 (4)	-2912 (10)

to $6s7s$ (^1S), the other 17 levels to $6s7s$ (^3S). Below the energy range of 45000 cm^{-1} we expect four additional levels contributing to the configuration $4f^{12}6s7s$ which have not yet been discovered experimentally: three characterized as (^1S) and one (^3S). The level assignments are accentuated by the good agreement between the experimental and calculated g-factors, also compiled in Table 4. The two levels, 37014.608 cm^{-1} ($J = 4$) and 36883.886 cm^{-1} ($J = 5$), demonstrate the strongest deviation in the g-factors. Therefore, at least these two levels seem to be incompletely addressed by the one-configuration description and demonstrate, as shown in the next sections, difficulties when included in the description of the hfs (however, not in JJ-coupling) and IS.

3.2 Isotope shift

The experimentally determined IS of the transitions compiled in Table 1 for the four Er isotope pairs $^{170-168}$Er, $^{170-167}$Er, $^{170-166}$Er, and $^{170-164}$Er are documented in Table 5 (the isotope shift values for the line at 646.540 nm could not be determined on grounds of worse signal to noise ratio). Including the IS results of transitions of the type $4f^{12}6s^2$ to $4f^{12}6s6p$ from [22–24], we were able to obtain the level IS for the nine levels of configuration $4f^{12}6s7s$ relative to the ground state, *i.e.* the level isotope shift of $^3H_6$ in $4f^{12}6s^2$ is defined as 0 MHz. The residual level isotope shifts (RLIS) are compiled in Table 6. Here, the contribution of the normal mass shift have been already subtracted. Table 7 presents the different contributions of the field shift (FS) and specific mass shift (SMS)

Table 6. Residual level isotope shifts (RLIS) including the experimental uncertainty (standard deviation) in brackets in the configuration $4f^{12}6s7s$ compiled for altogether four different Er isotope pairs: $^{170-168}$Er, $^{170-167}$Er, $^{170-166}$Er, and $^{170-164}$Er.

Energy cm^{-1}	Residual Level Isotope Shift (RLIS) in MHz			
	170-168	170-167	170-166	170-164
31719.664	-584.2 (1.1)	-953 (3)	-1159.8 (1.3)	-1740 (2)
31946.417	-583.2 (0.8)	-951 (2)	-1163.3 (1.0)	-1741 (3)
32218.588	-629.2 (1.5)	-1003 (4)	-1255.3 (1.4)	-1890 (4)
36883.886	-448.1 (1.8)	-720 (8)	-893 (2)	-1349 (4)
37014.608	-267.6 (1.9)	-424 (8)	-537 (3)	-809 (11)
37144.092	-703.1 (1.8)	-1147 (9)	-1398 (2)	-2089 (8)
38870.770	-626 (5)	-1004 (18)	-1249 (5)	-1879 (14)
38893.172	-608 (5)	-970 (20)	-1210 (6)	-1826 (17)
38921.185	-594 (3)	-948 (13)	-1187 (4)	-1786 (13)

Table 7. Field, specific mass and normal mass shift of nine investigated levels of $4f^{12}6s7s$ for the isotope pair $^{170-168}$Er only.

Level energy cm^{-1}	Field shift MHz	Specific mass shift MHz	Normal mass shift MHz
31719.664	-511 (6)	-73 (5)	36.5
31946.417	-511 (6)	-73 (5)	36.8
32218.588	-306 (4)	-323 (2)	37.1
36883.886	-310 (7)	-131 (5)	42.4
37014.608	-137 (7)	-131 (5)	42.5
37144.092	-572 (7)	-131 (5)	42.7
38870.770	-422 (8)	-204 (3)	44.8
38893.172	-404 (8)	-204 (3)	44.8
38921.185	-390 (6)	-204 (3)	44.8

in the RLIS for the isotope pair $^{170-168}$Er. The different IS contributions were determined from a King-diagram analysis [25] of the RLIS in Table 6, taking the residual transition IS of the Er I line at $\lambda = 605.279$ nm as reference [9] (the SMS is practically non-existent in this transition). Quite peculiar is the large variety in FS in Table 7 for the levels around 37000 cm^{-1}, leading to the clearly more positive RLIS of the levels 37014 and 36884 cm^{-1} than the average RLIS in Table 6. The FS in the term around 38900 cm^{-1} remains around -400 MHz. Note also the increasing SMS contribution at higher levels. The SMS equals -73 MHz for the lowest term (with the exception of the level at 32219 cm^{-1}, demonstrating a sudden increase in the SMS = -323 MHz), increases to -130 MHz in the middle term, and finally reaches -204 MHz at the highest investigated term. Typical for this situation, the SMS contributions are all negative, however, much larger than expected [26].

To investigate the possible influence of higher-order effects in the IS we followed the discussion made in [5]. The level IS $\Delta T^i_{\rm IS}$ of the configuration $4f^{12}6s7s$ can be expressed for each (pure) level i by the following equation:

$$\Delta T^i_{\rm RLIS} = d_{6s7s} + c^i_{4f} z_{4f} + c^i_{3,6s} g_3(f,6s) + c^i_{3,7s} g_3(f,7s). \quad (1)$$

The level IS can be divided into several different contributions, very similar to the theoretical description of the fs levels. The parameter d_{6s7s} stands for the common IS contributions in all levels. Any possible J-dependent effects in the IS are described by the parameter z_{4f}. The $g_{3,ns}(f,ns)$ parameters characterize second-order IS-effects of the FS and SMS (no discrimination), taking account possible term-dependent effects. The angular coefficients c^i_{4f}, $c^i_{3,6s}$ and $c^i_{3,7s}$ of the corresponding fs-integrals ζ_{4f}, $G^3(4f,6s)$ and $G^3(4f,7s)$ are taken from our fs-calculation of $4f^{12}6s7s$. Table 8 compiles the determined CSO-parameters of this study for the isotope pairs $^{170-168}$Er and $^{170-166}$Er on the basis of a least squares fit using equation (1). The correlation between the CSO-parameters $g_{3,6s}(f,6s)$ and $g_{3,7s}(f,7s)$ is extremely strong, *i.e.* the corresponding angular coefficients are so similar, that an individual determination was impossible. This problem reflects the difficulties that were encountered already during the fs-calculations for $G^3(4f,6s)$ and $G^3(4f,7s)$: a significant discrimination between the $6s$ and $7s$ electron contribution was not possible. Therefore, we can present only the result for the complete contribution $(g_{3,6s}(f,6s)+g_{3,7s}(f,7s))$. In addition, all three levels around 37000 cm^{-1} had to be excluded from our fit. Inside this term the deviations between the best fit values of the RLIS and the experimental RLIS for $^{170-166}$Er were all greater then 150 MHz. These levels seem to be disturbed by neighboring terms from other configurations. The z_{4f} parameter we obtained from the fit is practically equal 0 leading to the conclusion that any J-dependency in the IS is proven to be insignificant in this configuration. This result agrees very well with similar CSO evaluation of the IS performed for the equivalent configuration $4f^76s7s$ in Eu I: there the z_{4f} parameter also turned out to be zero [18]. The best fit values of the residual level isotope shift (RLIS) for isotope pair $^{170-166}$Er are compiled in the second column of Table 9 for the assigned 18 levels and the four experimentally unidentified levels. For four different levels the agreement is better than 5 MHz, which is within the range of our experimental uncertainty. The other two levels included for this fit demonstrate a slightly larger deviation of *ca.* 30 MHz which is acceptable.

Table 8. CSO-parameters of the reduced level isotope shift in the Er I configuration $4f^{12}6s7s$; Δ fit.: standard deviation between experimental and calculated reduced level isotope shifts.

CSO-Parameter	170-168Er MHz	170-166Er MHz
d_{6s7s}	-740 (30)	-1500 (50)
z_{4f}	2 (4)	3 (8)
$g_3(f,6s)+g_3(f,7s)$	-24 (15)	-50 (30)
Δ fit.	12	23

3.3 Hyperfine structure

3.3.1 In JJ-coupling

The assignment of the levels of the configuration $4f^{12}6s7s$ are given in [16] to terms in the JJ-coupling scheme $\left\{4f^{12}\left(^{2S_1+1}L_{1J_1}\right)6s7s\left(^{1,3}S_{J_2}\right)\right\}J$. In the special case that J_1 and J_2 are good quantum numbers the hfs-constants A and B can be expressed in the following very simple and straightforward non relativistic manner [2]:

$$A = \frac{1}{2J(J+1)} \times \Big((J(J+1)+J_1(J_1+1)-J_2(J_2+1))A(4f^{12}\alpha J_1) + (J(J+1)+J_2(J_2+1)-J_1(J_1+1))A(6s7s\beta J_2)\Big) \quad (2a)$$

$$B = \frac{3}{(2J+3)(2J+2)} \times \left(\frac{k_1(k_1+1)-4/3J(J+1)J_1(J_1+1)}{J_1(2J_1-1)}B(4f^{12}\alpha J_1) + \frac{k_2(k_2+1)-4/3J(J+1)J_2(J_2+1)}{J_2(2J_2-1)}B(6s7s\beta J_2)\right) \quad (2b)$$

$$k_1 = J_2(J_2+1)-J(J+1)-J_1(J_1+1);$$

$$k_2 = J_1(J_1+1)-J(J+1)-J_2(J_2+1).$$

$A(4f^{12}\alpha J_1)$ and $A(6s7s\beta J_2)$ characterize the contributions of the $4f^{12}$ and the combined $6s7s$ electron shells to the magnetic dipole hyperfine interaction, $B(4f^{12}\alpha J_1)$ and $B(6s7s\beta J_2)$ to the electric quadrupole hyperfine interaction. One can expect that $B(6s7s\beta J_2)$ converts to zero for a combined $6s7s$ electron shell. However, we did not want to omit the last part of the expression in equation (2b) in order to inspect if our data would underline this belief.

The levels of the configuration $4f^{12}6s7s$, for which experimental hfs-data exists, belong to the three terms $^3H_6\ ^3S_1$, $^3F_4\ ^3S_1$ and $^3H_5\ ^3S_1$. Following [16] the terms $^3H_6\ ^3S_1$ and $^3H_5\ ^3S_1$ are more then 98% pure in this JJ-coupling scheme, but the levels assigned to the term $^3F_4\ ^3S_1$ have a share of about 70% of this term only and an admixture of about 20% of $^1G_4\ ^3S_1$. About the remaining 10% no information is given in [16]. Because the angular coefficients for the hfs parameters are determinable only on the basis of the quantum numbers J_1, J_2 and J there is no possibility to distinguish between the parameters of $^3F_4\ ^3S_1$ and $^1G_4\ ^3S_1$, which have the same J_1 and J_2, *i.e.* (4, 1). So the levels of $^3F_4\ ^3S_1$ can be treated as 90% pure (4, 1).

Altogether four parameters of the magnetic dipole hyperfine interaction, $A(J_1 = 6, 5, 4)$ and $A(J_2 = 1)$, and four of the electric quadrupole hyperfine interaction, $B(J_1 = 6, 5, 4)$ and $B(J_2 = 1)$, were estimated by least squares fit procedure of equations (2a, 2b) on the basis of the experimental hfs-constants given in Table 2. The standard deviation between experimental and best fitted $A(J_1J_2)$ and $B(J_1J_2)$ is 16 MHz and 147 MHz respectively, equivalent to *ca.* 5% deviation towards the mean absolute value of the hfs-constants. Column 3 and 5 of Table 9 present the calculated hfs-constants using the outlined approach in JJ-coupling. The deviations to the experimental values are practically equally distributed. No level had to be excluded from the fit of either $A(J_1J_2)$ or $B(J_1J_2)$, an indication for the good description in JJ-coupling.

Table 10 compiles the resulting hfs-constants $A(J_1)$, $A(J_2)$ and $B(J_1)$, $B(J_2)$, representing the contribution of their shell. The main contribution in the magnetic dipole interaction is given by the combined $6s7s$-shell. For all levels with known experimental A-factors in a very good approximation the $6s7s$-shell can be described as $^3S_1$ base term. $A(J_2 = 1)$ is then equals $0.5(a^{10}_{6s} + a^{10}_{7s})$, where a^{10}_{6s} and a^{10}_{7s} represent the relativistic one-electron hfs parameters of the two different s-electrons (in SL-coupling). This approximation leads to a total s-shell contribution of $a^{10}_{6s} + a^{10}_{7s} = 2A(J_2 = 1) = -1780(100)$ MHz to the magnetic

Table 9. Calculated residual level isotope shifts $RLIS_{\rm cal}$ for the isotope pair $^{170-166}$Er, magnetic dipole and electric quadrupole constants, $A_{\rm calc}$ and $B_{\rm calc}$ respectively in the configuration $4f^{12}6s7s$ in MHz, theoretical modeling in LS-coupling (2nd, 4th and 6th column) and in JJ-coupling (3rd and 5th column) – further details see text; Δ: difference between calculated and experimental values. Slanted energy values: experimental location unknown.

	LS-coupling-scheme		*JJ*-coupling-scheme		*LS*-coupling-scheme		*JJ*-coupling-scheme		*LS*-coupling-scheme	
level	$RLIS_{cal}$	Δ	A_{calc}	Δ	A_{calc}	Δ	B_{calc}	Δ	B_{calc}	Δ
cm^{-1}	MHz	MHz	MHz	MHz	MHz	MHz	MHz	MHz	MHz	MHz
***J* = 1**										
44886.482	-1172				231				529	
***J* = 2**										
44347.866	-1180				113				726	
45060.489	-1179				-219				838	
***J* = 3**										
37144.092	-1235	{-163}	70	30	91	9	19	231	341	-91
42611.413	-1185				30				-1190	
44308.935	-1196				-200				891	
45246.857	-1161				-410				1541	
***J* = 4**										
37014.608	-1188	{651}	-160	-3	-172	9	30	-136	446	{-552}
38685	-1194				-84				352	
38921.185	-1223	36	-2	2	4	-4	-3367	-73	-3290	-150
42681.708	-1203				-184				-2111	
44192	-1154				-317				822	
44401	-1296				-181				-1991	
***J* = 5**										
32218.588	-1251	4	-3	22	25	-6	-3745	-272	-3923	-94
36883.886	-1178	{285}	-276	13	-217	8	23	-2	594	{-573}
38893.172	-1209	-1	-175	5	-174	4	-3541	-44	-3526	-59
40488	-1197				-144				-3900	-
42736.803	-1247				-311				-2448	-
***J* = 6**										
31946.417	-1162	1	-148	-14	-152	-10	-3875	69	-3974	168
33519.739	-1248				-88				-4293	
38870.770	-1217	-32	-273	-6	-275	-4	-4050	100	-3931	-19
***J* = 7**										
31719.664	-1163	3	-239	8	-226	-5	-4271	76	-4299	104

Table 10. Hfs splitting constants $A(J_1)$, $A(J_2)$, $B(J_1)$ and $B(J_2)$ of the configuration $4f^{12}6s7s$ in JJ-coupling, determined from the fit of the experimental hfs constants in Table 2a using equations (2a, 2b).

Hfs constant	Value in MHζ
$A(J_1 = 4)$	- 122 (12)
$A(J_1 = 5)$	- 150 (40)
$A(J_1 = 6)$	-130 (7)
$A(J_2 = 1)$	- 890 (50)
$B(J_1 = 4)$	30 (100)
$B(J_1 = 5)$	- 4900 (300)
$B(J_1 = 6)$	- 5020 (100)
$B(J_2 = 1)$	0 (80)

dipole interaction. If one assumes an insignificant contribution of the $7s$ electron the result then for the $6s$ electron alone compares very well with $a^{10}_{6s} = -1635(35)$ MHz from the Er I configuration $4f^{12}5d6s6p$ [12] and with $a^{10}_{6s} = -1891(2)$ MHz from Er II configuration $4f^{12}6s$ [27].

The magnetic dipole parameters $A(J_1 = 6, 5, 4)$ of the different core states of the $4f^{12}$ shells are very similar, averaging at about -135 MHz. Opposite to this, we obtained a large variety in the electric quadrupole parameters in the different core states of $4f^{12}$, $B(J_1 = 6, 5, 4)$, depending strongly on the electronic arrangement of the $12f$ electrons. The electric quadrupole parameter $B(J_1 = 4)$ for $^3F_4$ is insignificant, while the constants $B(J_1 = 6, 5)$ of the $^3H_{J_1}$ terms are around -5000 MHz. The fit also demonstrated that $B(J_2 = 1)$ equals 0 MHz, as was expected: the s-electrons do not contribute to an electric quadrupole moment in first order approximation. The results for $B(J_1 = 6, 5, 4)$ remained in the frame of uncertainty when the fit was performed with $B(J_2 = 1)$ defined as zero. In conclusion, this instructive non-relativistic hfs-interpretation in JJ-coupling reproduced the experimental hfs constants in all nine levels of $4f^{12}6s7s$ very well.

3.3.2 In SL-coupling

To be able to evaluate tendencies on the basis of hfs parameters from other electronic configurations, we re-examined the hfs in the SL-coupling scheme. Hence, to determine the relativistic one-electron parameters, we calculated the four magnetic dipole and three electric quadrupole parameters in a configuration of the type $4f^n6s7s$ in the effective operator technique following [2]:

$$A = \alpha^{10}_{4f}a^{10}_{4f} + \alpha^{01}_{4f}a^{01}_{4f} + \alpha^{12}_{4f}a^{12}_{4f} + \alpha^{10}_{6s}a^{10}_{6s} + \alpha^{10}_{7s}a^{10}_{7s} \quad (3a)$$

and

$$B = \beta^{02}_{4f}b^{02}_{4f} + \beta^{11}_{4f}b^{11}_{4f} + \beta^{13}_{4f}b^{13}_{4f}. \quad (3b)$$

The corresponding angular coefficients, α^{kl}_{4f} and β^{kl}_{4f}, were calculated using the program *chfs* [28]. The admixtures

Table 11. Hfs (relativistic) one-electron parameters (in MHz) for the configuration $4f^{12}6s7s$ in neutral ^{167}Er, deduced from the measured hyperfine constants using the wavefunctions of the fine structure calculations in LS-coupling. *: Parameter values related to the corresponding a^{01} and b^{02} as described in text.

One-electron hfs-parameter	Value in MHζ
a^{10}_{4f}	**7.9 ***
a^{01}_{4f}	**-147 (3)**
a^{12}_{4f}	**-160 ***
$a^{10}_{6s} + a^{10}_{7s}$	**- 1840 (30)**
b^{02}_{4f}	**6580 (80)**
b^{11}_{4f}	**-505 ***
b^{13}_{4f}	**940 ***

of the SL-states are given by our fs analysis. The relativistic one-electron parameters were estimated by least squares fit procedure of equations (3a, 3b). Due to the strong linear correlation of the parameters and the fact that the hfs constants were determined for nine levels only, it was necessary to reduce the number of free one-electron parameters from 5 to 2 for the magnetic dipole and from 3 to 1 for the electric quadrupole. In each case, two parameters of the $4f$-shell remained in a fixed ratio to one left free, as outlined in [11]. Table 11 compiles the relativistic one-electron parameters, of which a^{01}_{4f}, $\{a^{10}_{6s} + a^{10}_{7s}\}$, and b^{02}_{4f}, were determined independently. We tried to solve the $6s$ and $7s$ magnetic dipole contributions separately. This was, however, impossible, for reasons similar as outlined in the evaluation of the IS and fs. Table 9 compiles the experimental and theoretical hfs-constants $A_{\rm calc}$ and $B_{\rm calc}$ for all the classified levels of $4f^{12}6s7s$. The fit is characterized by a standard deviation of 10 MHz for A and 145 MHz for B. We did again recognize difficulties for the two levels 37015 cm^{-1} and 36884 cm^{-1}. The recalculated electric quadrupole moment for both levels demonstrated a very strong deviation of over 500 MHz, see Table 9. The agreement between experimental and recalculated magnetic dipole moments is good, even for the apparently disturbed levels at 37015 cm^{-1} and 36884 cm^{-1}. Therefore, they were excluded from the fit for the electric quadrupole constants, but not for the magnetic dipole constants.

4 Discussion

The evaluation of the IS and the hfs gives us some indication of the source for the disturbance in the levels at 37000 cm^{-1}. The configuration mixing into these levels of $4f^{12}6s7s$ is affecting the IS and the electric quadrupole constant, without noticeably changing the expected magnetic dipole constant. This leads us to conclude that the main configuration involved in the mixing is $4f^{12}5d6s$. The $6s$ electron contributes to most of the magnetic dipole moment, so a mixture with this configuration would show

Table 12. Experimental hfs radial parameters a^{10}_{ns} in MHz and corresponding radial integrals $\langle r^{-3}\rangle^{10}_{ns}$ in a.u. for configurations with open $6s$ and $7s$ shells for the lanthanides Eu, Gd, Er and Tm.

Isotope	configuration	a^{10}_{6s}	a^{10}_{7s}	$a^{10}_{6s}+a^{10}_{7s}$	$\langle r^{-3}\rangle^{10}_{6s}+\langle r^{-3}\rangle^{10}_{7s}$	ref.
^{151}Eu	$4f^7\,6s7s$	11870(90)	1950(90)	13820(180)	105.3(1.4)	[18]
^{157}Gd	$4f^7\,5d6s7s$	-2053(12)	-395(11)	-2448(23)	113.3(1.0)	[30]
^{167}Er	$4f^{12}\,6s7s$			-1840(30)	121(2)	this work
^{169}Tm	$4f^{13}\,6s7s$	-5058(47)	-1012	-6070(60)	138.9(1.4)	[17]
^{173}Yb	$4f^{14}\,6s7s$			-3758(20)	144.3(8)	[32]*

* $a^{10}_{6s}+a^{10}_{7s}$ derived from $^{173}A(^3S_1)$

no appreciable effect on the A-factors. However, the interaction of the $5d$-electron with the $4f^{12}$-shell is severely different and could alter any theoretical IS and electric quadrupole constant for a pure level of $4f^{12}6s7s$ significantly. Reinspection of the experimentally determined even levels in Er I [16] leads to the following: two unclassified levels that lie very close (less than 17 cm^{-1}) to the disturbed ones, namely 36997 cm^{-1} ($J = 4$) and 36898 cm^{-1} ($J = 5$). The highest classified level of the configuration $4f^{12}5d6s$ is at 33750.645 cm^{-1}, almost 90% of the even parity levels above that energy range remain unclassified. We propose to assign these two levels 36997 cm^{-1} ($J = 4$) and 36898 cm^{-1} ($J = 5$) as predominantly $4f^{12}5d6s$.

That the constants B of the disturbed levels 37014 cm^{-1} and 36883 cm^{-1} match well for the fit in JJ-coupling can be explained by the fact that a free parameter $B(J_1 = 4)$ is used to fit the B values for this term.

To compare the results of the parametric analysis of the hfs of configurations with open $6s$ and $7s$ shells for different lanthanides, the one-electron parameters a^{10}_{ns} are transformed to the radial integrals $\langle r\rangle^{10}_{ns}$ using the following expression [29]:

$$\langle r\rangle^{k_s k_l}_{nl} = 0.010481\ \frac{I}{\mu_I}\ a^{k_s k_l}_{nl}$$

where $a^{k_s k_l}_{nl}$ is given in MHz, $\langle r\rangle^{k_s k_l}_{nl}$ in units of a_0^{-3}, I is the nuclear spin and μ_I the nuclear moment in units of nuclear magnetons. Data are available for the five lanthanides Eu, Gd, Er, Tm and Yb and are collected in Table 12. For Gd the corresponding configuration is $4f^7 5d6s7s$, where one $6s$ electron of the ground configuration is excited to the $7s$-shell. The parameter a^{01}_{4f} do not appear for Eu, Gd and Yb, either due to the restriction of the $4f^7$ to the ^8S core state or due to the closed $4f$-shell. Therefore, a discussion of the parameter of the $4f$ shell is discarded. Since in three cases the total contribution of the $6s7s$ shells is determined only, we confine to this parameter.

Europium

The sub-configuration $4f^7(^8S)6s7s$ of Eu consists of four levels only, their A constants have been determined experimentally [18]. Due to the restriction of the $4f^7$ to the ^8S core state the contribution of the $4f$-electron is expressed by the single parameter a^{10}_{4f}. For Eu it was possible to estimate independently the contribution of the $6s$ and the $7s$ electron from a least squares fit with three parameters and four A constants [18]. The ratio of a^{10}_{6s}/a^{10}_{7s} is equal to 6.1.

Gadolinium

The main problem in Gd is the large number of hfs parameters due to the open $5d$ electron shell, although (for the same reason as for Eu) the contribution of the $4f$-electron is expressed by one single parameter only. Using the experimental A constants for ten levels the parameter a^{10}_{7s} has been determined [30]. But the Fermi contact terms of the $4f$, $5d$ and $6s$ shells are strongly correlated and only one single common radial parameter $A^{10}_{4f,5d,6s}$ results from the fit. Since the contribution of the $6s$ shell strongly dominates and the contribution of the $4f$ and $5d$ shell is estimated to be in the order of the uncertainties, the parameter a^{10}_{6s} is set equal to $A^{10}_{4f,5d,6s}$ [30]. Then the ratio of a^{10}_{6s}/a^{10}_{7s} is equal to 5.2.

Erbium

For Er it was not possible to determine the contributions of $6s$ and $7s$ separately, although the experimental hfs constants are determined for nine levels. This is due to the fact that all these nine levels are mainly composed of $6s7s(^3S)$ states (see above). Therefore, a separation of the contribution of the $6s$ and the $7s$ with these states is impossible.

Thulium

The configuration $4f^{13}6s7s$ of Tm consists of nine levels. The A constants of all these levels are known [17,31]. In principle it is possible to determine the ratio a^{10}_{6s}/a^{10}_{7s} on the basis of this experimental hfs data. However, the ratio decisively depends on the wave functions of the four ^3S levels with $J = 5/2$ and $7/2$, which on the other hand depend on the ratio between the fine structure parameters $G^3(4f, 6s)$ and $G^3(4f, 7s)$. This ratio $G^3(4f, 6s)/G^3(4f, 7s)$ may be varied from 5 to 20 without any appreciable influence on the standard deviation of the fit. Therefore, for Tm the only statement, that can be made for this ratio a^{10}_{6s}/a^{10}_{7s} is, that it lies between 5 and 20 [17].

Ytterbium

The configuration $4f^{14}6s7s$ of Yb has a closed $4f$ shell and is composed of two levels only, one of these with $J = 0$. The A constant of the $^3S_1$ level is measured for example in [32] with $^{173}A = -1879(10)$ MHz. For this level the angular coefficients α^{10}_{ns} for the $6s$ and $7s$ shell are 0.5, that results in a value of $a^{10}_{6s} + a^{10}_{7s} = 3758(20)$ MHz.

For all five elements a variety of problems arise, but in all cases at least the common contribution of the $6s$

and $7s$ shell to the hfs can be determined. The five values of the radial integrals $\langle r^{-3}\rangle_{6s}^{10} + \langle r^{-3}\rangle_{7s}^{10}$ increase with the nuclear charge of the elements and lie pretty well on a straight line. This indicates the increase in binding energy of the ns electrons with increasing nuclear charge due to the imperfect shielding of the $4f$ electrons. The same trend was found for the s electrons in other configurations of the lanthanides (see for example [3]). The ratio a_{6s}^{10}/a_{7s}^{10} could be determined in two cases and estimated in one. It is in all three cases in the same order of magnitude.

5 Conclusion

Here, the hyperfine splitting constants A and B and the residual level isotope shift for nine levels of the configuration $4f^{12}6s7s$ have been determined experimentally. A parametric analysis of the level IS values and of the A and B factors in JJ- and SL-coupling are performed. With exceptions of two levels at around 37000 cm^{-1} the experimental values could be well reproduced by the fits and theoretical predictions for the experimentally unknown A and B constants and the residual level isotope shift could be stated. The discrepancy of the values for the two levels at 37000 cm^{-1} can be explained by energetic near lying perturbing levels. A comparison of the parameter a_{6s}^{10} with values of the Er I configuration $4f^{11}5d6s6p$ and of the Er II configuration $4f^{12}6s$ shows good agreement.

The present work is part of a systematic investigation of isotope shift and hyperfine structure of elements in the series of lanthanides.

We would like to acknowledge our student D. Knoblauch for the help in the experiments and J.-F. Wyart (Orsay, France) for the many advises concerning the fine structure calculations. One of us [D.A.] would also like to thank M. Wilson (London, England) for the stimulating discussions.

References

1. P.G.H. Sandars, J. Beck, Proc. R. Soc. Lond. A **289**, 97 (1965).
2. L. Armstrong Jr, *Theory of Hyperfine Structure of Free Atoms* (Wiley-Interscience, New York, London, Sydney, Toronto, 1971).
3. V. Pfeufer, Z. Phys. D **4**, 351 (1987).
4. J. Bauche, R.-J. Champeau, Adv. At. Mol. Phys. **12**, 39 (1976).
5. H.-D. Kronfeldt, G. Klemz, D.-J. Weber, J. Phys. B: At. Mol. Opt. Phys. **23**, 1107 (1990).
6. V. Pfeufer, W.J. Childs, L.S. Goodman, J. Phys. B **16**, L557 (1983).
7. W.J. Childs, L.S. Goodman, V. Pfeufer, Phys. Rev. A **28**, 3402 (1983).
8. H.-D. Kronfeldt, D. Ashkenasi, H. Nikseresht, Z. Phys. D **22**, 569 (1992).
9. H. Brüggemeyer, V. Pfeufer, U. Nielsen, J.-F. Wyart, Z. Phys. D **1**, 269 (1986).
10. W.-J. Childs, L.S. Goodman, K.T. Cheng, Phys. Rev. A **33**, 1469 (1986).
11. H.-D. Kronfeldt, D. Ashkenasi, S. Kröger, J.-F. Wyart, Phys. Scripta **48**, 688 (1993).
12. H.-D. Kronfeldt, G. Klemz, S. Kröger, J.-F. Wyart, Phys. Rev. A **48**, 4500 (1993).
13. S. Kröger, J.-F. Wyart, P. Luc, Phys. Scripta **55**, 579 (1997).
14. S. Kröger *et al.*, Z. Phys. D **25**, 185 (1997).
15. S. Held, N. Spector, Israel Atomic Energy Commision, Soreq. Nuc. Res. Center, IA-1345-T (1980) and IA-1385, IA-1385-T (1983).
16. W.C. Martin, R. Zalubas, L. Hagan, *Atomic Energy Levels - The Rare Earth Elements*, edited by W.C. Martin, R. Zalubas, L. Hagan, Natl. Bur. Stand. (U.S.) Na. Go. (U.S. GPO, Washington DC, 1978).
17. H.-D. Kronfeldt, S. Kröger, Z. Phys. D **34**, 219 (1995).
18. J.R. Kropp, H.-D. Kronfeldt, R. Winkler, Z. Phys. A **321**, 365 (1985).
19. H.-D. Kronfeldt, D. Ashkenasi, G. Basar, L. Neale, M. Wilson, Z. Phys. D **25**, 185 (1993).
20. H.-D. Kronfeldt, D. Ashkenasi, G. Klemz, in *LASER 92*, edited by C.P. Wang (STS-Press, Mc. Lean, 1993), p. 676.
21. H.-D. Kronfeldt, G. Klemz, D. Ashkenasi, Opt. Commun. **110**, 549 (1994).
22. D. Ashkenasi, Ph.D. thesis, Technische Universität Berlin, ISBN 3-929937-89-1, Verlag Köster, Berlin, 1994.
23. W.G. Jin, T. Horiguchi, M. Wakasugi, Y. Yoshizawa, J. Phys. Soc. Jpn **59**, 3148 (1990).
24. H. Brüggemeyer, Ph.D. thesis, Universität Hannover, 1987.
25. W.S. King, *Isotope Shift in the Atomic Spectra* (Plenum Press, N.Y., 1984).
26. K. Heilig, A. Steudel, *New Developments of Classical Optical Spectroscopy*, Progress in Atomic Spectroscopy, edited by W. Hanle, H. Kleinpoppen (Plenum Press New York and London, 1978).
27. U. Nielsen, K.T. Cheng, H. Ludvigsen, J.N. Xiao, Phys. Scripta **34**, 776 (1986).
28. S. Kröger, M. Kröger, Comput. Phys. Commun. **90**, 381 (1995).
29. S. Büttgenbach, *Hyperfine Structure in 4d- and 5d-Shell Atoms* (Springer-Verlag Berlin, Heidelberg, New York, 1982).
30. G. Klemz, H.-D. Kronfeld, S. Kröger, paper in preparation.
31. Y. Bordarier, R. Vetter, J. Blaise, J. Phys. **24**, 1107 (1963).
32. R.W. Berends, L. Maleki, Opt. Soc. Am. B **9**, 332 (1992).